Available online at www.sciencedirect.com
ScienceDirect
Journal of Power Sources 171 (2007) 457–463
JOURNAL OF POWER SOURCES
www.elsevier.com/locate/jpowsour

Direct water balance analysis on a polymer electrolyte fuel cell (PEFC): Effects of hydrophobic treatment and micro-porous layer addition to the gas diffusion layer of a PEFC on its performance during a simulated start-up operation

Hironori Nakajima*, Toshiaki Konomi, Tatsumi Kitahara

Department of Mechanical Engineering Science, Faculty of Engineering, Kyushu University, 744 Motooka, Nishi-ku, Fukuoka 819-0395, Japan

Received 25 January 2007; received in revised form 26 May 2007; accepted 4 June 2007
Available online 13 June 2007

Abstract

Effects of hydrophobic treatment and micro-porous layer (MPL) addition to a gas diffusion layer (GDL) in a polymer electrolyte fuel cell (PEFC) have been investigated from water balance analysis at the electrode (catalyst layer), GDL and flow channel in the cathode after a simulated start-up operation. The water balance is directly analyzed by measuring the weight of the adherent water wiped away from each the component. As a result, we find that hydrophobic treatment without MPL leads to the increase in liquid water accumulation at the electrode which limits the oxygen transport to the catalyst and then lowers the cell voltage rapidly during start-up, whereas the treatment decreases the water at the GDL. The water accumulation at the electrode also decreases the cumulative current that represents the power generation and calorific power indispensable for warming up at a temperature below freezing point. On the other hand, we directly find that the hydrophobic treatment with MPL addition suppresses the water accumulation at the electrode, which increases the cumulative current. In addition, it is found that increase in air permeability of a GDL substrate by its coarser structure increases the cumulative current, which is explained by enhancing the exhaust of the product water vapor and liquid as well as by enhancing the oxygen transport directly. Thus, the hydrophobic treatment with MPL addition and larger air permeability of a GDL substrate improve the start-up performance of a PEFC.

Keywords: PEMFC; Gas diffusion layer; Hydrophobic treatment; micro-porous layer; Water balance; Start-up

1. Introduction

Polymer electrolyte fuel cell (PEFC) is promising as a zero emission power source for future automobiles and houses because PEFC generates electricity from hydrogen (H_2) and oxygen (O_2) exhausting only water. Proper water management at the electrode (catalyst layer), gas diffusion layer (GDL), and flow channels of a PEFC is necessary to improve its performance since the flooding due to the liquid product water accumulated at the electrode, GDL and flow channel lowers the performance while supplying dry gas leads to the lowering of the performance by decreasing the proton conductivity of the proton exchange membrane (PEM).

The rapid exhaust of the product water has been of significant interest for the improvement of the cell performance by suppressing the flooding, which is particularly required to avoid the freezing of the water during the start-up of a PEFC at a temperature below freezing point. The rapid exhaust is necessary to realize reliable PEFC systems for the automobiles and houses since the sufficient power generation by the rapid exhaust enables their efficient warming up to prevent the freezing of the product water [1–3] while the exhaust enables the removal of the water before it freezes in the cell.

We have therefore investigated the exhaust of the product water in terms of the mechanism of the plug flow in the flow channel by *in situ* observation using a transparent PEFC combined with the analysis of the change of the cell voltage

* Corresponding author. Tel.: +81 92 802 3160; fax: +81 92 802 0001.
E-mail address: nakajima@mech.kyushu-u.ac.jp (H. Nakajima).

0378-7753/$ – see front matter © 2007 Elsevier B.V. All rights reserved.
doi:10.1016/j.jpowsour.2007.06.004

in our previous paper [4]. In the present paper, we focus on the effects of hydrophobic treatment and micro-porous layer (MPL) addition [5] to a GDL substrate on the flooding. There have been researches on their effects on the cell performance so far [6–8]. We have also investigated their effects on the concentration overpotential [9]. Thus, we aim to investigate their effects on the amount of the liquid water accumulated at each the component of the cell directly and separately during a simulated start-up operation. The amount of the water accumulated at each the component have not been measured separately although the total amount have been measured [10]. In addition, we investigate the cumulative current during the start-up operation since it determines the power generation and calorific power in the start-up. The calorific power is especially important to warm up a PEFC at a temperature below freezing point.

2. Water balance in a PEFC

In the anode of a PEFC, water is transported into by the humidified hydrogen and the back-diffusion in the membrane while transported out by the electro-osmotic drag and exhausted hydrogen. In the cathode, water is transported into by the humidified air, the production by reaction, and the electro-osmotic drag while transported out by the exhausted air and the back-diffusion. The water content in the membrane is determined by the above balance. It follows that the liquid water accumulates at the electrode, GDL, and flow channel. Here, we focus on the water accumulated in the cathode that mainly determines the performance of a PEFC.

3. Experimental

3.1. Apparatus

All measurements were performed using a PEFC as shown in Fig. 1. The clamp load of the cell was variable with monitoring by a load cell (LCN-A-2KN, Kyowa Electronic Instruments Co., Ltd.). Bipolar plates were made of graphite and had flow fields of parallel channels, whose width and depth were 0.8 and 0.5 mm, respectively. All the channels were connected by four intersecting channels. A membrane electrode assembly (MEA) (PRIMEA 5510, Japan Gore-Tex Inc., catalyst: 0.3 mg Pt cm^{-2}at each side, thickness: 30 μm, geometrical area of electrodes: 13 cm^2) was sandwiched between paper type gas diffusion layers (GDLs) (SIGRACET GDL 20AA/20BA/20BC/21BC, SGL Carbon Inc.) described later. The clamp load of the cell was adjusted at 1000 N (0.77 MPa) that was determined from the result of our previous papers [11,12] to prevent the damage from creep and to obtain a stable performance. Thereby the clamp load was identical for all the GDLs.

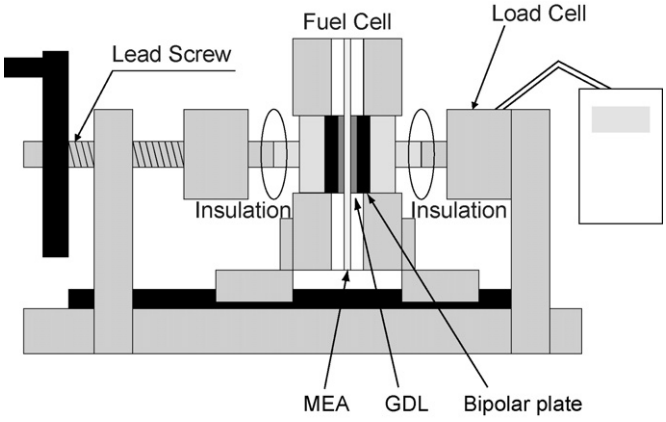

Fig. 1. Schematic illustration of the fuel cell with the variable clamp load mechanism.

Pure H_2 and dried air were supplied into the anode and cathode lines, respectively, at a constant flow rate so that the stoichiometric ratios in both sides were 2 at the current density of 1 A cm^{-2}.

The temperature of the cell was maintained at 40 ° C using circulating water through a thermostatic bath (NTB-221, Tokyo Rikakikai Co., Ltd.) since we have empirically observed tendency that the most drastic lowering of the cell performance by the flooding around 40 ° C under start-up operation so far. The flooding is suppressed below 40 ° C owing to the small amount of the product water ascribed to the small current density. The flooding is also suppressed above 40 ° C since the major part of the product water is rapidly exhausted in the form of vapor.

Both the anode and cathode gases were humidified at 40 ° C using a fuel cell test system (890-G1S, TOYO Corp.) so that the relative humidity of the supplied gases were both 100%.

Current-voltage (*I–V*) curves were obtained with an electronic load system (890 C, Scribner Associates, Inc.) controlled by a personal computer. Ohmic resistances of the cell were measured by current interrupter method using the same system to obtain IR losses.

3.2. Gas diffusion layer

The properties of GDLs used are summarized in Table reproduced by the courtesy of SGL Carbon Inc. The number 20 or 21 represents the areal weight of a plain GDL substrate, which determines the air permeability of the GDL substrate. The number 20 is for a standard type while 21 type is coarser and has the areal weight about 2/3 of that of 20 type to increase the permeability. The character A or B following the number represents the GDL substrate without or with hydrophobic treatment by 5 wt% PTFE (polytetrafluoroethylene) loading hydrophobic treatment, respectively. The last character A or C is for the GDL substrate without or with the MPL addition, respectively. The hydrophobic treatment and the MPL addition increase the electrical resistance of the GDL by 5 and 4 Ω cm^{-2}, respectively. The Gurley number that is a measure of the air permeability and defined as the time required for a fixed volume (100 cm^3) of gas to pass through a fixed area of film (6.42 cm^2) at a constant pressure difference using a prescribed apparatus [13,14] becomes approximately 1/80 by the MPL addition. The permeability of the GDL 21BC is 3.6 times larger than that of GDL 20BC.

Table 1
Design parameters of paper type GDLs

Material	Thickness (μm)	PTFE content (wt%)	MPL addition	Air permeability ($cm^3\,cm^{-2}s^{-1}$)	Areal weight ($g\,m^{-2}$)	Electrical resistance ($m\,\Omega\,cm^2$)
GDL 20AA	215	0	No	50	60	<5
GDL 20BA	220	5	No	50	65	<10
GDL 20BC	260	5	Yes	0.65	110	<14
GDL 21BC	260	5	Yes	2.35	95	<15

This table is reproduced by the courtesy of SGL Carbon Inc.

3.3. Simulated start-up operation

We carried out the simulated start-up operation as follows:

Step 1. Dried nitrogen gas was introduced into the cell at the flow rate of 500 $cm^3\,min^{-1}$ for 4 h to dry the cell. Then we dismantled the cell and confirmed that no liquid water water remained at the electrode and flow channels.
Step 2. The cell was assembled with a new GDL.
Step 3. The cell was maintained at open circuit voltage (OCV) for 5 min.
Step 4. The cell was maintained at OCV for 2 min.
Step 5. Current density was increased by 25 mA $cm^{-2}\,s^{-1}$. Cell voltage and IR loss were recorded for each current density.
Step 6. When the cell voltage reaches 0.35 V, the current density was decreased by 25 mA $cm^{-2}\,s^{-1}$ per second until the cell voltage reaches OCV.

We repeated the cycle of the Steps 4–6 20 times.

3.4. Direct measurement of the weight of accumulated water

The weight of the GDL was measured before and after the start-up operation. The weight of the GDL after the start-up operation was measured as quickly as possible. The amount of the accumulated water at the GDL was estimated by the difference of the weight. The amounts of water accumulated at the electrode and flow channel were directly evaluated by measuring the weight of the adherent water carefully wiped away with a cotton applicator. The amounts of the adherent water at the electrode and GDL were not so large as to cause uncertain water movement between the electrode and GDL during dismantling. Thus, we regard that the change of the water distribution and behavior at the cathode electrode and GDL is negligible.

The amount of water vapor in the supplied and exhausted air were evaluated from the measurement of the humidity and temperature of the supplied air at the inlet and outlet of the cell using a thermohygrometer (HygroClip IC-1 with HygroFlex 32D, ROTRONIC AG Corp.). The change of the amount of the water in the membrane was estimated from the change of the IR loss of the cell.

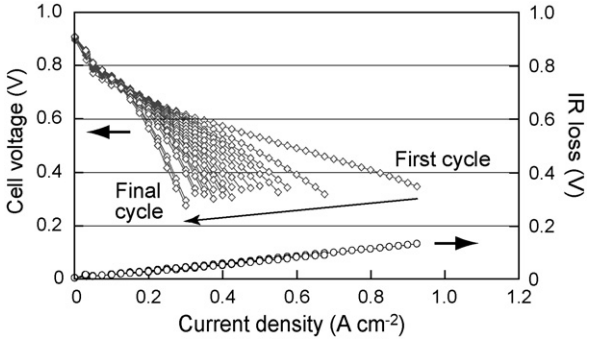

Fig. 2. *I–V* curves and IR losses of the PEFC with the GDL 20AA during the start-up operation at 40 °C. Relative humidity : 100%.

4. Results and discussion

4.1. I–V curves

4.1.1. The standard GDL 20AA

Fig. 2 shows the *I–V* curves and IR loss for the GDL 20AA, i.e. a plain GDL substrate. As the cycle of the Steps 4–6 is repeated, the drop of the cell voltage increases, which is significant after the second and third cycle. Since the change of the IR loss is small, the increase in the water in the membrane is negligible. The increase in the drop of the cell voltage is explained by the product water accumulated at the electrode and GDL that limits the transport of O_2 to the catalyst.

4.1.2. GDL substrate with hydrophobic treatment, 20BA

Fig. 3 shows the *I–V* curves and IR loss for the GDL substrate with the hydrophobic treatment (GDL 20BA). The *I–V*

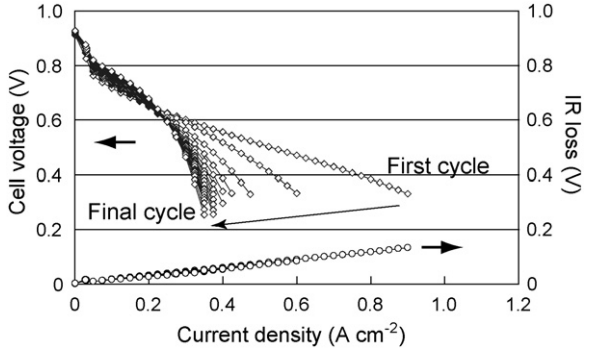

Fig. 3. *I–V* curves and IR losses of the PEFC with the GDL 20BA during the start-up operation at 40 °C. Relative humidity : 100%.

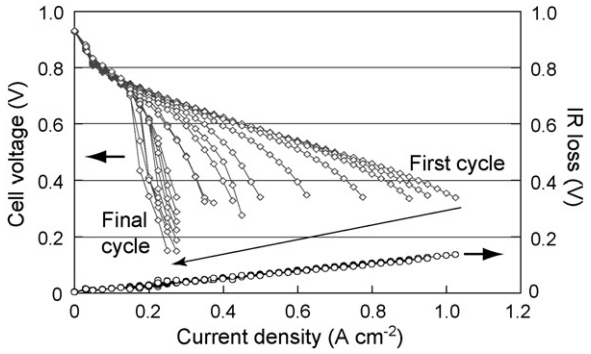

Fig. 4. *I–V* curves and IR losses of the PEFC with the GDL 20BC during the start-up operation at 40 °C. Relative humidity : 100%.

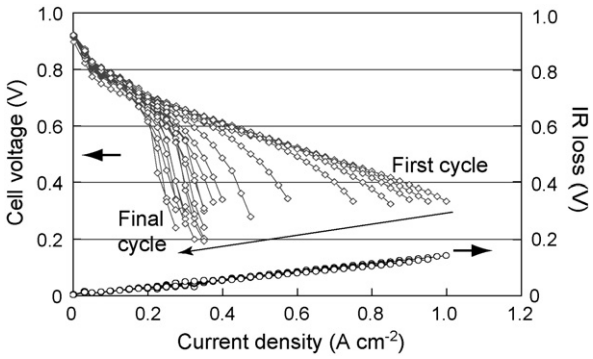

Fig. 5. *I–V* curves and IR losses of the PEFC with the GDL 21BC during the start-up operation at 40 °C. Relative humidity : 100%.

characteristics do not change by the treatment for the first cycle with respect to the case of the GDL 20AA. Small amount of the cumulative water for both the case is possibly responsible for this accordance. However, the drop of the cell voltage is larger after the second cycle. Since the hydrophobic treatment decreases the accumulated water at the GDL by repelling the condensed water at the GDL to the electrode and flow channel, the larger drop is due to the accumulated water at the electrode, which limits the transport of O_2 to the catalyst. The *I–V* curve finally becomes almost the same. The small amount of the cumulative water ascribed to the small cell voltage possibly results in decrease in the adherent water at the GDL despite the larger amount of that at the electrode. Thus, the oxygen transport rate finally becomes almost the same as the case of the GDL 20AA. IR loss is also almost the same as the case of the GDL 20AA.

4.1.3. GDL substrate with hydrophobic treatment and MPL addition, 20BC

Fig. 4 shows *I–V* curve and IR loss for the GDL substrate with the hydrophobic treatment and MPL addition (GDL 20BC). The *I–V* characteristics do not change by the hydrophobic treatment and MPL addition for the first cycle compared with the case of the GDL 20AA and GDL 20BA. This is explained by the same reason as the case of the GDL 20AA and GDL 20BA. However, the drop of the cell voltage is smaller after the second cycle compared with the case of the former GDLs. Thus, the accumulated water at the electrode is shown to decrease by the MPL. The drop of the cell voltage finally becomes larger since the cumulative product water is larger owing to the larger cumulative current that possibly increases the adherent water at the flow channel and lowers the oxygen transport rate, taking into account the small amount the water at the GDL from the analysis of the adherent water at each component shown later. IR loss is almost the same as the case of the former GDLs.

4.1.4. GDL having small areal weight with hydrophobic treatment and MPL addition, 21BC

Fig. 5 shows *I–V* curve and IR loss for the GDL substrate having smaller areal weight that leads to larger air permeability with hydrophobic treatment and MPL addition. The cell voltage during the first cycle is almost the same as the case of the GDL 20BC. However, the drop of the cell voltage is smaller than the case of the GDL 20BC as the cycle is repeated, indicating larger cumulative current. IR loss is almost the same as the case of the former GDLs, although the resistance of 21BC is 1 m $\Omega\,cm^2$ larger than that of the GDL 20BC.

4.2. Adherent water and cumulative product water

Fig. 6 shows the weight of the adherent water wiped away from the electrode, GDL, and flow channel after the twenty cycles during the start-up operation for the GDL 20AA, GDL 20BA, and GDL 20BC. For the case of the GDL 20AA, for instance, the weights of the water are approximately 20, 70, and 50 mg for the electrode, GDL, and flow channel, respectively. These results are compared with the amount of the cumulative product water (CPW), W_{CPW}, calculated from the cumulative current using the following equation.

$$W_{CPW} = \frac{M_{H_2O} A}{2F} \int i\,dt \quad (1)$$

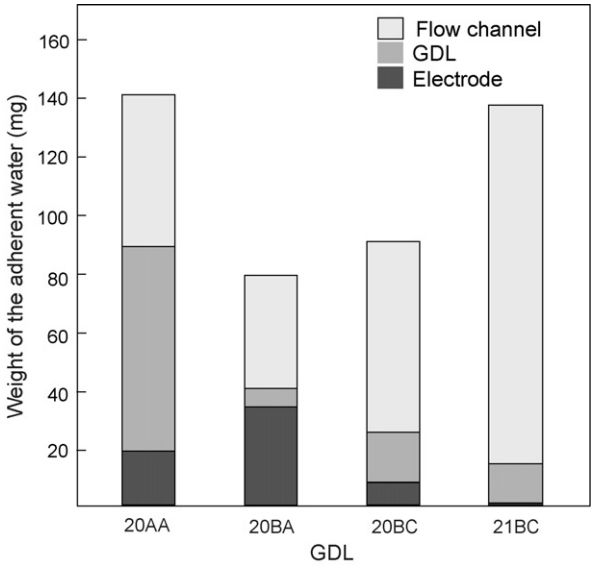

Fig. 6. Weight of the adherent water wiped away from the electrode, GDL, and flow channel of the PEFC with the GDL 20AA, GDL 20BA, GDL 20BC, and GDL 21BC during the start-up operation at 40 °C. Relative humidity: 100%.

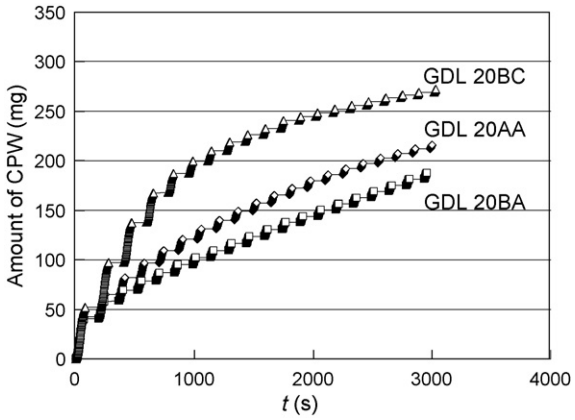

Fig. 7. Transient of cumulative product water in the PEFC with the GDL 20AA, GDL 20BA, and GDL 20BC during the start-up operation at 40 °C. Relative humidity : 100%.

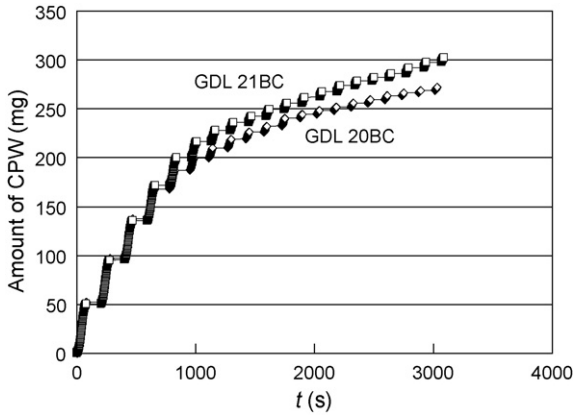

Fig. 8. Transient of the cumulative product water in the PEFC with the GDL 20BC and GDL 21BC during the start-up operation at 40 °C. Relative humidity : 100%.

where M_{H_2O} denotes the molar weight of water, A the geometrical area, i is the current density on the basis of the geometrical area. F and t have their common meanings. The cumulative current is discussed using W_{CPW} hereafter for the comparison.

Fig. 7 shows W_{CPW} for the GDL 20AA, GDL 20BA, and GDL 20BC. For the case of the GDL 20AA, W_{CPW} from Eq. (1) is approximately 40 mg during the first cycle. The amount of CPW is constant at the OCV for 2 min (Step 4) and increases during the twenty cycles, while the increment of W_{CPW} becomes smaller as the cycle is repeated.

The amount of CPW for the GDL 20AA during the start-up operation calculated from Eq. (1) is 80 mg larger than the sum of the weight of the water for the GDL 20AA of 140 mg. The difference is mainly ascribed to the water transported out in the form of liquid water from the flow channel since both the water content in the vapor in the exhausted air at the cathode inlet/outlet and IR loss that represents the water content in the PEM were unchanged during the operation. Accordingly, further study on the amount of the exhausted liquid water needs to be performed to consider the adherent water at the flow channel. Thus, we concentrate on the adherent water at the electrode and GDL in the present paper.

For the case of the GDL 20BA, W_{CPW} for the first cycle is almost the same as the case of the GDL 20AA. As the cycle is repeated, the CPW increment for one cycle is smaller than the case of the GDL 20AA. After the final cycle, W_{CPW} for the GDL 20BA is approximately 20% smaller than the case of the GDL 20AA. For each the component, the weight of the adherent water at the GDL 20 BA is approximately 1/9 of that at the GDL 20AA as shown in Fig. 6, which results from the hydrophobic treatment. However, the weight of the adherent water at the electrode is twice as large as that for the GDL 20AA. The water seems to accumulate mainly at the electrode and flow channel for the case of the GDL 20BA.

For the case of the GDL 20BC, W_{CPW} is rather larger than the case of the GDL 20AA and GDL 20BA until the 10th cycles and becomes almost the same as the case of the GDL 20AA and GDL 20BA after the 10th cycle. The amount of CPW after twenty cycles is 20% larger and 40% larger than that for the GDL 20AA and GDL 20BA, respectively. For each the component, the weight of the adherent water at the GDL 20BC is approximately four times larger than that for the GDL 20BA, while that at the electrode is approximately 1/6 of that for the GDL 20BA.

Fig. 8 shows W_{CPW} of the GDL 20BC and GDL 21BC. The difference becomes large after the fifth cycle. Finally, W_{CPW} for the GDL 21BC becomes 10% larger than that for the GDL 20BC. The weight of the adherent water at the GDL 21BC is 3/4 of that at the GDL 20BC. Almost no liquid water is obtained at the electrode for the case of the GDL 21BC, whereas the weight of the adherent water at the flow channel is twice as large as that for the GDL 20BC.

4.3. Determinant of the cumulative product water

The above results show that the hydrophobic treatment decreases W_{CPW}, whereas the treatment with MPL addition increases it. Moreover, the larger permeability of the GDL substrate is shown to increase the W_{CPW}. In this section, we discuss the determinant of the W_{CPW}. Here, we focus on the effects of the liquid water volume ratio in the total GDL pore volume and average water thickness at the electrode on the W_{CPW} from the viewpoint of the comparison of the effects between the liquid water at the electrode and GDL.

We firstly examined the relation between W_{CPW} and the water volume ratio at the GDL as shown in Fig. 9. The pore volume of the GDL substrate is calculated from its specific gravity, the weight of the PTFE for the hydrophobic treatment, and the volume of the GDL substrate. It can be seen from Fig. 9 that the W_{CPW} decreases as the increase in the ratio of the water except for the GDL 20BA. However, such exception shows that the ratio is not the major determinant.

Secondly, we examined the relation between W_{CPW} and the average water layer thickness at the electrode which is calculated form the weight of the adherent water at the electrode as shown in Fig. 10. The amount of CPW decreases as the increase in the average water layer thickness. The major determinant of W_{CPW} is thus indicated to be the average water layer thickness.

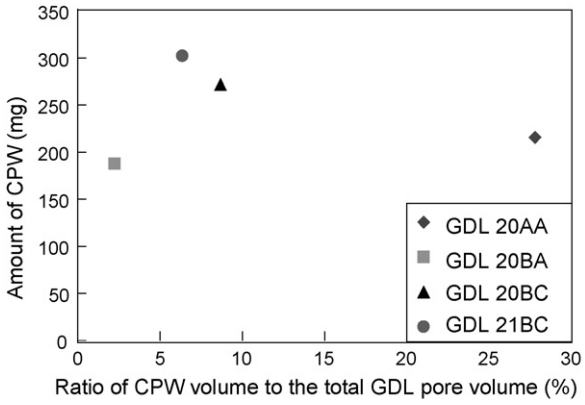

Fig. 9. Relation between the cumulative product water and its volume ratio in the total GDL pore volume in the PEFC with the GDL 20AA, GDL 20BA, GDL 20BC, and GDL 21BC during the start-up operation at 40 °C. Relative humidity: 100%.

We then examined the above two factors quantitatively by the multiple correlation analysis. As the result, the contribution from the average water layer thickness was 0.95, while that from the water volume ratio was 0.03. The average water layer thickness was statistically significant at 5% level since its significance probability is 0.015. These results support that the major determinant of W_{CPW} is the average water layer thickness.

The product water mainly accumulates at the electrode and flow channel for the case of the GDL substrate with the hydrophobic treatment (GDL 20BA). The amount of the adherent water at the electrode is larger than the case without the hydrophobic treatment (GDL 20AA). The hydrophobic treatment decreases the accumulated water at the GDL because the liquid water condensed in the GDL is easily repelled toward the electrode and flow channel owing to the treatment. The larger drop is thus due to the accumulated water at the electrode, which limits the transport of O_2 to the catalyst. This also results in the increase in the concentration overpotential, and decrease in the cell voltage and the cumulative current. The increase in the water layer thickness accordingly decreases W_{CPW}. However, the hydrophobic treatment presumably effective for the transport of the water from the GDL to the flow channel.

On the other hand, for the case of the hydrophobic treatment with MPL addition (GDL 20BC), the amount of the adherent water at the electrode is smaller than the case with only the hydrophobic treatment (GDL 20BA) owing to the MPL, whereas the amount at the GDL is larger. The decrease in the water layer thickness accordingly increases W_{CPW}. The water is produced in the form of vapor at the electrode and transported through the MPL to the flow channel. Then a part of the vapor water condenses at the electrode and GDL. The MPL is likely to prevent the transport of the liquid water at the GDL to the electrode.

The increase in the air permeability of the GDL substrate (GDL 21BC) results in the decrease in the adherent water at the electrode and GDL, and increase in the water at the flow channel. This is explained by increase in the vapor exhausted to the flow channel from the electrode through the MPL and from the liquid water condensed at the GDL. Coarse GDL substrate structure that leads to the large air permeability also enhances the removal of the condensed water at the GDL in the form of liquid. Thus, the increase in the air permeability of the GDL substrate by its coarser structure is effective for slowing increase in the voltage drop by enhancing the exhaust of the vapor and liquid water as well as by directly enhancing the transport of the O_2 to the catalyst, leading to the increase in W_{CPW} during start-up.

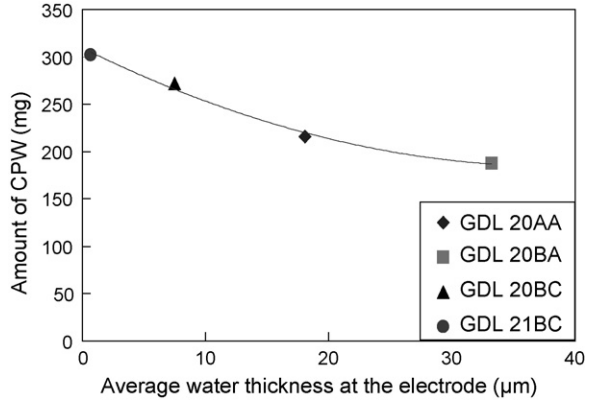

Fig. 10. Relation between the cumulative product water and the average water thickness on the electrode in the PEFC with the GDL 20AA, GDL 20BA, GDL 20BC, and GDL 21BC during the start-up operation at 40 °C. Relative humidity: 100%.

5. Conclusion

We directly analyze the dependence of the amount of the water accumulated in each the component of a PEFC during the start-up operation on the hydrophobic treatment and MPL addition to a GDL substrate by measuring the weight of the adherent water at each the component at 40 °C.

The hydrophobic treatment without MPL addition results in further water accumulation at the electrode compared with the case without any treatment. Accordingly, the increase in the water layer thickness at the electrode decreases the cumulative current and cumulative product water. On the other hand, the hydrophobic treatment with MPL addition results in the increase in the cumulative current and cumulative product water owing to the suppress of the water accumulation at the electrode with respect to the case without any treatment. Hence, the hydrophobic treatment with MPL addition is directly shown to be effective to improve the start-up performance of a PEFC by suppressing the water accumulation at the electrode. Increase in the air permeability of the GDL substrate by its coarser structure is also effective for the improvement since it enhances the exhaust of the product water in the form of vapor and liquid. In addition, the transport of the O_2 to the catalyst is directly enhanced by the increase in the air permeability.

Acknowledgements

This study was partly supported by the grant of the 21st century center of excellence (COE) program “Integration Tech-

nology of Mechanical Systems for Hydrogen Utilization" from the Japanese Ministry of Education, Culture, Sports, Science and Technology (MEXT) and by the grant of the partnership project "Hydrogen Technology Research" from MEXT and Fukuoka prefecture, Japan.

References

[1] Y. Hishinuma, T. Chikahisa, F. Kagami, T. Ogawa, JSME Int. J. Ser. B Fluids Therm. Eng. 47 (2004) 235–241.
[2] M. Oszcipok, M. Zedda, D. Riemann, D. Geckeler, J. Power Sources 154 (2006) 404–411.
[3] T. Hottinen, O. Himanen, P. Lund, J. Power Sources 154 (2006) 86–94.
[4] T. Konomi, G. Nakamura, Trans. Jpn. Soc. Mech. Eng. Part B 72 (2006) 745–751.
[5] M. Mathias, J. Roth, J. Fleming, W. Lehnert, W. Vielstich, A. Lamm, H.A. Gasteiger, Handbook of Fuel Cells: Fundamentals Technology and Applications, vol. 3, John Wiley & Sons, Ltd., New York,2003.
[6] Z. Qi, A. Kaufman, J. Power Sources 109 (2002) 38–46.
[7] G. Lin, T. Van Nguyen, J. Electrochem. Soc. 152 (2005) A1942–A1948.
[8] A. Weber, J. Newman, J. Electrochem. Soc. 152 (2005) A677–A688.
[9] T. Konomi, T. Kitahara, Y. Sasaki, Trans. Jpn. Soc. Mech. Eng. Part B 72 (2006) 758–763.
[10] T. Fabian, J. Posner, R. O'Hayre, S.-W. Cha, J. Eaton, F. Prinz, J. Santiago, J. Power Sources 161 (2006) 168–182.
[11] T. Kitahara, T. Konomi, Y. Sasaki, Trans. Jpn. Soc. Mech. Eng. Part B 72 (2006) 752–757.
[12] T. Kitahara, T. Konomi, Trans. Jpn. Soc. Mech. Eng. Part B 72 (2006) 1007–1012.
[13] Japanese Standards Association, JIS P 8117, 1998.
[14] International Organization for Standardization, ISO 5636/5, 1986.